Astragaloside IV suppresses triple-negative breast cancer cell migration and invasion by targeting BCAT1-mediated branched-chain amino acid metabolism

YI-TING LIU, LU ZHANG and XIAO-DONG SUN

Department of Medical Oncology, Yan'an University Affiliated Hospital, Yan'an, Shaanxi 716000, P.R. China

Received December 18, 2025; Accepted June 25, 2026

DOI: 10.3892/ol.2026.15796

Abstract. Branched-chain amino acid (BCAA) transaminase 1 (BCAT1), the rate-limiting enzyme in BCAA metabolism, serves a pivotal role in tumor progression. Astragaloside IV (AS-IV) exhibits potential antitumor properties; however, whether AS-IV suppresses breast cancer migration by modulating BCAA metabolism via BCAT1 remains to be elucidated. The present study aimed to investigate whether AS-IV inhibits the invasion and migration of MDA-MB-231 triple-negative breast cancer (TNBC) cells by targeting BCAT1-mediated BCAA metabolic reprogramming. The present study used network pharmacology to predict AS-IV targets against breast cancer invasion, followed by BCAT1 knockdown and overexpression in MDA-MB-231 cells. Using molecular docking, cellular thermal shift assay, wound healing, Transwell, western blotting, quantitative PCR and liquid chromatography-mass spectrometry metabolomics, the present study systematically evaluated: i) AS-IV-BCAT1 direct binding and protein stability; ii) BCAA metabolic flux regulation via the branched-chain α-ketoacid dehydrogenase kinase (BCKDK)/branched-chain α-ketoacid dehydrogenase (BCKDH) axis; and iii) functional impacts on breast cancer cell migration and invasion. Network pharmacology predicted BCAT1 as a key potential target of AS-IV, with significant enrichment of the BCAA metabolic pathway. The results of the present study suggested that AS-IV binds to and stabilizes BCAT1 *in vitro*, an effect that is associated with reduced migration and invasion of MDA-MB-231 cells. It also promotes BCAA degradation via the BCKDK/BCKDH axis, lowering intracellular BCAA levels and suppressing malignancy. Notably, AS-IV maintained dose-dependent inhibition even with BCAT1 knockdown or overexpression, albeit with reduced efficacy. In conclusion, the present study suggested that AS-IV suppresses MDA-MB-231 cell invasion and migration by targeting BCAT1-mediated BCAA metabolism. These findings support further evaluation of AS-IV in TNBC and highlight BCAA metabolism as a potential intervention point in future research.

Correspondence to: Dr Xiao-Dong Sun, Department of Medical Oncology, Yan'an University Affiliated Hospital, 43 North Road, Yan'an, Shaanxi 716000, P.R. China
E-mail: yasxd680522@163.com

Abbreviations: BCAA, branched-chain amino acid; BCAT1, BCAA transaminase 1; AS-IV, astragaloside IV; BCKDK, branched-chain α-ketoacid dehydrogenase kinase; BCKDHB, branched-chain keto acid dehydrogenase E1 subunit β; CETSA, cellular thermal shift assay; TNBC, triple-negative breast cancer

Key words: AS-IV, BCAT1, breast cancer, mechanism

Introduction

Breast cancer remains the most common malignancy among women worldwide (1) and the leading cause of cancer-related deaths in women, with an estimated 2.3 million new cases and 670,000 deaths globally in 2022 (2,3). Although notable progress has been made in early diagnosis and comprehensive treatment strategies, tumor migration continues to be the primary cause of treatment failure and patient mortality (4,5). The invasion and migration of tumor cells constitute a multi-step complex process, involving metabolic reprogramming, epithelial-mesenchymal transition and remodeling of the tumor microenvironment (6). Among these, metabolic dysregulation, an emerging hallmark of cancer, serves a key role in providing precursors for macromolecular synthesis and maintaining redox homeostasis. In particular, dysregulated amino acid metabolism has been closely associated with malignant tumor progression (7).

Branched-chain amino acids (BCAAs), including leucine, isoleucine and valine, serve not only as key substrates for protein synthesis but also as notable signaling molecules and energy sources (8). BCAA metabolism is frequently dysregulated in cancer and the key enzyme BCAA transaminase 1 (BCAT1) has been implicated in tumor progression (9). BCAT1 catalyzes the initial step of BCAA catabolism, sustaining intracellular BCAA reserves to fuel anabolic processes such as mTOR signaling and nucleotide synthesis (8,9). In breast cancer, BCAT1 is upregulated in aggressive subtypes including triple-negative breast cancer (TNBC) and this upregulation is associated with poor prognosis (10). Specifically, immunohistochemical analysis of breast cancer tissue microarrays in a previous study confirmed that high BCAT1 expression is associated with

higher histological grade (Nottingham grading system), lymph node migration and worse prognosis (11). Functional studies have demonstrated that BCAT1 promotes breast cancer cell proliferation, migration and invasion, partly by activating mTOR signaling and sustaining intracellular BCAA reserves (11,12), with emerging evidence implicating downstream pathways such as SHOC2-Ras-ERK in TNBC (13). BCAT1 has also been associated with endocrine therapy resistance; specifically, its upregulation sustains the proliferation of antiestrogen-resistant and estrogen receptor (ER)α^- breast cancer cells (12).

However, despite these advances, key knowledge gaps remain regarding the oncogenic functions and underlying mechanisms of BCAT1 in TNBC, particularly its contribution to migration through metabolic reprogramming (10,12,13). To the best of our knowledge, the majority of mechanistic studies have focused on ER^+ models, and the specific role of BCAT1 in TNBC migration, particularly its contribution through metabolic reprogramming, has not been fully elucidated. Notably, whether pharmacological targeting of BCAT1-mediated BCAA metabolism can suppress TNBC progression has not been explored, to the best of our knowledge. Due to the potent pro-metastatic functions of BCAT1 in TNBC, identifying agents that modulate BCAT1 activity and BCAA metabolism may offer novel therapeutic opportunities in the future.

Astragalus membranaceus, a traditional Chinese medicine that is believed to reinforce vital energy and enhance immune function, contains the active ingredient astragaloside IV (AS-IV), which has been demonstrated to possess diverse pharmacological activities including immunomodulatory, anti-inflammatory, antioxidant and antitumor effects (14-16). Recent studies have suggested that AS-IV can inhibit proliferation, invasion and induce apoptosis in multiple types of cancer cell, including hepatocellular carcinoma, nasopharyngeal carcinoma, oral cancer, ovarian cancer, gastric cancer and triple-negative breast cancer (17-23). Nevertheless, whether AS-IV exerts antitumor effects through the modulation of tumor metabolism, particularly amino acid metabolic pathways, remains to be elucidated.

The concept of network pharmacology was first proposed by the British scholar Andrew L. Hopkins in 2007 (24). This discipline integrates biology systems, traditional pharmacology computer network science, systems biology, bioinformatics and network science. Based on a systems-level perspective and a holistic view of biological networks, network pharmacology elucidates the molecular connections between drugs and diseases, clarifies drug therapeutic mechanisms and provides guidance for novel drug development and clinical practice (25). The analytical methods of network pharmacology for target genes align well with the multi-component, -target and -mechanism characteristics of traditional Chinese medicine, making it a current research hotspot in the field (26-30). Molecular docking technology, by contrast, is a computer-aided drug design method. The core mechanism lies in embedding small molecule compounds into macromolecular structures, aiming to predict interactions between 'target-ligand' and 'structure-activity' at the molecular level. Molecular docking technology is extensively applied in predicting the efficacy of novel compounds, exploring polypharmacology and drug repurposing (31-33).

Among breast cancer subtypes, TNBC is particularly aggressive, lacks targeted therapies and is associated with poor prognosis. Increasing evidence suggests that BCAA metabolism may be particularly key in TNBC, as these tumors exhibit metabolic vulnerabilities distinct from hormone receptor or HER2-amplified subtypes (12,34,35). Therefore, as an initial exploration of whether AS-IV exerts anti-metastatic effects through BCAT1-mediated BCAA metabolism, the present study focused on the MDA-MB-231 TNBC cell line as a representative and clinically relevant model.

Building upon this background, we hypothesized that AS-IV suppresses the invasive and migratory capabilities of MDA-MB-231 TNBC cells and that this effect may involve BCAT1-mediated reprogramming of BCAA metabolism. This hypothesis was derived from network pharmacology predictions, which identified multiple potential targets of AS-IV associated with breast cancer. BCAT1 was prioritized for experimental validation based on three criteria: i) BCAT1 ranked among the top core targets in the protein-protein interaction (PPI) network based on degree centrality; ii) pathway enrichment analysis demonstrated notable involvement of the BCAA degradation pathway; and iii) emerging evidence suggests BCAA metabolism serves a key role in TNBC progression (10,12,13); however, whether AS-IV modulates this pathway has not been explored. Notably, although previous studies have reported the antitumor effects of AS-IV in various cancer types, its direct targeting of a metabolic enzyme, particularly BCAT1, has not yet been demonstrated. Thus, the present study, to the best of our knowledge, represents the first attempt to associate AS-IV with BCAT1-mediated BCAA metabolic reprogramming in breast cancer cells. Specifically, the present study aimed to investigate this hypothesis and further explore the underlying molecular mechanisms, with a focus on examining whether AS-IV interacts with BCAT1 to modulate BCAA metabolism in TNBC cells. The findings may provide a theoretical basis for further investigation of AS-IV in metabolic intervention strategies against breast cancer migration in the future.

Materials and methods

Experimental materials

Cell source. The MDA-MB-231 TNBC cell line [American Type Culture Collection (ATCC)® HTB-26™] was obtained from the ATCC. All cells were cultured in high-glucose DMEM medium (cat. no. 11965084; Gibco; Thermo Fisher Scientific, Inc.) supplemented with 10% fetal bovine serum (cat. no. 30-2020; ATCC) and 1% penicillin/streptomycin at 37˚C under 5% CO_2.

Reagents. AS-IV (purity, ≥98%; cat. no. S1101-01019) was purchased from Nanjing Jingzhu Biotechnology Co., Ltd. The rabbit polyclonal antibody against BCAT1 (cat. no. ab197941) was acquired from Abcam. Lipofectamine® 3000 transfection reagent was obtained from Thermo Fisher Scientific, Inc. BCAT1-specific small-interfering RNA (siRNA/si) and non-targeting negative control (NC) siRNA, BCAT1 overexpression (OE) plasmid (pcDNA3.1-BCAT1) and empty vector were synthesized by Shanghai GenePharma Co., Ltd. Matrigel matrix was procured from Corning, Inc. The Seahorse XF Cell Energy Metabolism Assay Kit (cat. no. 103325-100) was

sourced from Agilent Technologies, Inc. BCAA standards (leucine, isoleucine and valine) and isotopic internal standards were purchased from MilliporeSigma.

Network pharmacological analysis

Screening of drug and disease targets. Potential targets of AS-IV were identified using databases including SwissTargetPrediction (based on 2D and 3D similarity measures; http://www.swisstargetprediction.ch/), Similarity Ensemble Approach Search Server (based on set-wise chemical similarity among ligands; https://sea.bkslab.org/), PharmMapper (based on reverse pharmacophore mapping; https://www.lilab-ecust.cn/pharmmapper/), SuperPred (based on machine learning and 2D similarity; https://prediction.charite.de/subpages/target_prediction.php) and TargetNet (based on Naïve Bayes QSAR models; http://targetnet.scbdd.com/calcnet/index/). Breast cancer-associated targets were retrieved from disease databases such as GeneCards (http://www.genecards.org/), Online Mendelian Inheritance in Man (OMIM; http://omim.org/) and Disease Gene Network (DisGeNET; https://disgenet.com/). The intersections of the drug and disease targets were selected as the candidate targets.

Screening of core targets for AS-IV in the treatment of breast cancer. The intersections between the obtained targets of AS-IV and the disease targets of breast cancer were identified using the Venny online platform (version 2.1.0; https://bioinfogp.cnb.csic.es/tools/venny/). This process yielded the potential therapeutic targets of AS-IV for breast cancer and a Venn diagram was generated accordingly.

PPI network construction and topological analysis. The potential therapeutic targets of AS-IV for breast cancer were imported into the Search Tool for Retrieval of Interacting Genes/Proteins database (https://string-db.org/). Under 'Multiple proteins' the 'Organisms' parameter was set to '*Homo sapiens*' to conduct PPI analysis and obtain PPI information, which was then saved in tab-separated values format. Subsequently, the data was imported into the Cytoscape software (version 3.10.0; https://cytoscape.org/) for visualization. Topological analysis was performed using the CytoHubba (version 1.6) and MCODE (version 2.0.3)plugins.

Gene Ontology (GO) and Kyoto Encyclopedia of Genes and Genomes (KEGG) enrichment analysis. To further characterize the roles of the potential targets of AS-IV in treating breast cancer in terms of gene function and signaling pathways, KEGG signaling pathway and GO functional enrichment analyses were performed on the potential therapeutic targets using the Metascape database (https://metascape.org; version 3.5.20260201). The enrichment analysis results were visualized via the bioinformatics online plotting platform (http://www.bioinformatics.com.cn/).

Construction of the 'AS-IV-core targets-key pathways-breast cancer' network. The top five entries from both the KEGG pathway and the GO functional enrichment analyses results were selected. The corresponding target data for these entries were collected. These targets, along with the files containing the intersecting targets between the drug and disease, were imported into the Cytoscape software (version 3.10.0; https://cytoscape.org/)) to construct the 'AS-IV-core targets-key pathways-breast cancer' network diagram.

Cell culture and treatment. MDA-MB-231 TNBC cells were routinely cultured in DMEM medium (cat. no. 11965084; Gibco; Thermo Fisher Scientific, Inc.) supplemented with 10% FBS (cat. no. 30-2020; ATCC) and 1% penicillin/streptomycin (cat. no. 15140122; Gibco; Thermo Fisher Scientific, Inc.). AS-IV was dissolved in DMSO to prepare a 20 mM stock solution, which was stored at -20˚C. For experiments, the stock was diluted to desired concentrations with serum-free medium, ensuring that the final DMSO concentration was not >0.1%.

Establishment of BCAT1 knockdown (KD) cell model. BCAT1 expression was knocked down using siRNA technology. In total, three specific siRNA sequences targeting BCAT1 and a non-targeting NC siRNA were designed and synthesized by Shanghai GenePharma Co., Ltd. The target sequences are presented in Table SI. MDA-MB-231 TNBC cells were seeded into 6-well plates ($5x10^5$ cells/well) and transfected at 60-70% confluence with 50 nM siRNA using Lipofectamine® 3000 (Thermo Fisher Scientific, Inc.) according to the manufacturer's instructions. Transfection was performed at 37˚C for 6 h, after which the medium was replaced with fresh complete medium. Cells were harvested 48 h post-transfection and KD efficiency was validated by western blotting and quantitative PCR (qPCR) as later described.

After screening, only si-BCAT1-1 exhibited a stable and notably efficient KD effect (the comparison of the three siBCAT1 KD sequences is presented in Fig. S1). Subsequent experiments were all conducted using this sequence (siBCAT1-1).

Establishment of BCAT1-overexpression cell model. The full-length BCAT1 complementary DNA (cDNA) was cloned into the pcDNA3.1 vector to construct the OE plasmid. The target sequence is presented in Table SI. The PCR product was digested and inserted into the pcDNA3.1(+) vector. The construct was verified by Sanger sequencing. Cell seeding and transfection procedures were performed as described in the previous section. Briefly, cells were transfected with 2.5 μg BCAT1 overexpression plasmid or empty vector per well using Lipofectamine® 3000 (Thermo Fisher Scientific, Inc.) at 37˚C for 6 h, after which the medium was replaced with fresh complete medium. OE efficiency was confirmed via western blotting and qPCR 48 h after transfection. Overexpression efficiency was confirmed via western blotting and quantitative PCR (qPCR) 48 h after transfection, as later described.

Validation of the binding interaction between AS-IV and BCAT1

Molecular docking. Molecular docking simulations were performed using the AutoDock Vina software (version 1.2.0; The Scripps Research Institute; https://vina.scripps.edu/). The crystal structure of BCAT1 (Protein Data Bank database identifier, 9BFA) was retrieved from the Protein Data Bank database (PDB; https://www.rcsb.org/). Water molecules and original ligands were removed using the PyMOL software (version 2.5.0; Schrödinger, LLC; https://pymol.org/); hydrogen atoms were added and charges were assigned. The 3D structure of AS-IV (compound identifier, 13943299) was obtained from the PubChem database (https://pubchem.ncbi.

nlm.nih.gov/) and energy-minimized. The docking grid was centered on the original ligand coordinates with a predefined box size. Default parameters were used for docking and the conformation with the lowest binding free energy was selected as the optimal binding mode. Protein-ligand interactions (for example, hydrogen bonds) were visualized using the PyMOL software.

Cellular thermal shift assay (CETSA). MDA-MB-231 TNBC cells were divided into control and AS-IV-treated groups (10 μM AS-IV for 24 h). Cells were collected and lysed in RIPA lysis buffer [50 mM Tris-HCl (pH 7.4), 150 mM NaCl, 1% NP-40, 0.5% sodium deoxycholate and 0.1% SDS; cat. no. P0013B; Beyotime Biotechnology] supplemented with protease and phosphatase inhibitors. The lysates were aliquoted and heated at temperatures ranging from 37˚C to 67˚C for 3 min. After centrifugation at 20,000 x g for 20 min at 4˚C, the supernatants were subjected to western blotting to examine changes in BCAT1 thermal stability, as later described.

Functional cell assays

Wound healing assay. Cells were seeded into 6-well plates at a density of $3x10^5$ cells/well and cultured to 90% confluence. A sterile 200 μl pipette tip was used to create a linear scratch across the cell monolayer. Detached cells were removed by gently washing twice with PBS. The medium was replaced with serum-reduced medium (DMEM containing 1% FBS) supplemented with various concentrations of AS-IV (0, 10, 20 and 40 μM). For each well, three pre-marked positions along the scratch were captured under an inverted microscope (Olympus CKX53; x10 objective; Olympus Corporation) at 0 and 24 h after scratching. The scratch area was quantified using ImageJ software (version 1.53; National Institutes of Health, Bethesda, MD, USA) by tracing the cell-free region. For each image, the wound area was measured in three independent regions and averaged.

Transwell invasion assay. Transwell inserts (8-μm pore size; 24-well format; Corning, Inc.) were coated with 50 μl of Matrigel matrix (diluted 1:8 in serum-free DMEM; Corning, Inc.) and allowed to solidify at 37˚C for 2 h. Cells from different treatment groups were harvested, washed twice with PBS and resuspended in serum-free DMEM. A total of $5x10^4$ cells in 200 μl serum-free medium were seeded into the upper chamber. The lower chamber was filled with 600 μl DMEM containing 10% FBS as a chemoattractant. After 24 h of incubation at 37˚C in 5% CO_2, non-invading cells on the upper surface of the membrane were carefully removed with a cotton swab. The inserts were then fixed with 4% paraformaldehyde for 20 min at room temperature, washed with PBS and stained with 0.1% crystal violet for 15 min at room temperature. After washing with distilled water and air-drying, invaded cells on the lower surface were imaged under an inverted light microscope (Olympus CKX53; x20 objective; Olympus Corporation). For each insert, five randomly selected fields were captured and the number of invaded cells was counted manually using the cell counter plugin in ImageJ software (version 1.53; National Institutes of Health). The average cell count per field was calculated for each insert. All experiments were performed with three independent biological replicates (n=3), each with three technical replicates (three inserts per condition).

Detection of BCAT1 and downstream protein expression

Western blotting. Total protein was extracted from three independent biological replicates per treatment group using RIPA lysis buffer [50 mM Tris-HCl (pH 7.4), 150 mM NaCl, 1% NP-40, 0.5% sodium deoxycholate and 0.1% SDS; cat. no. P0013B; Beyotime Biotechnology] supplemented with protease and phosphatase inhibitors. Protein concentration was quantified using the BCA method. Equal amounts of protein (30 μg per lane) from each biological replicate were separated on 10% gels using SDS-PAGE and transferred to PVDF membranes. After blocking with 5% bovine serum albumin (BSA; cat. no. A7030; MilliporeSigma) in TBST [20 mM Tris-HCl (pH 7.6), 137 mM NaCl and 0.1% Tween-20] for 1 h at room temperature, the membranes were incubated with specific primary antibodies (anti-BCAT1 rabbit polyclonal antibody: cat. no. ab197941; dilution 1:1,000; Abcam; and anti-β-actin mouse monoclonal antibody: cat. no. A5441; dilution 1:5,000; Merck KGaA) overnight at 4˚C. Subsequently, the membranes were incubated with HRP-conjugated secondary antibodies (goat anti-rabbit IgG-HRP: cat. no. 7074; dilution 1:2,000; Cell Signaling Technology, Inc.; and goat anti-mouse IgG-HRP: cat. no. 7076; dilution 1:2,000; Cell Signaling Technology, Inc.) for 1 h at room temperature. After thorough washing with TBST, protein bands were visualized using an ECL chemiluminescence substrate (Clarity™ Western ECL Substrate; cat. no. 1705061; Bio-Rad Laboratories, Inc.,) and imaged. β-actin was used as the internal control and band intensities were semi-quantified using ImageJ software (version 1.53; National Institutes of Health).

Reverse transcription-qPCR. Total RNA was extracted from three independent biological replicates per treatment group using TRIzol® reagent (cat. no. 15596018; Thermo Fisher Scientific, Inc.). RNA concentration and purity were measured using a NanoDrop™ 2000 spectrophotometer (Thermo Fisher Scientific, Inc.). cDNA was synthesized from 1 μg RNA per sample using the SuperScript® IV First-Strand Synthesis System (cat. no. 18091050; Thermo Fisher Scientific, Inc.) according to the manufacturer's protocol (25˚C for 5 min, 50˚C for 10 min and 80˚C for 10 min). qPCR was performed in triplicate technical replicates for each biological sample using specific primers and SYBR® Green Mix (iTaq™ Universal SYBR Green Supermix; cat. no. 1725121; Bio-Rad Laboratories, Inc.) on a Bio-Rad CFX96 real-time PCR system (under the following conditions: 95˚C for 30 sec; 40 cycles of 95˚C for 5 sec and 60˚C for 30 sec). The target sequences are presented in Table SI. β-actin was used as the reference gene and relative mRNA expression levels were calculated using the $2^{-\Delta\Delta Cq}$ method (36).

Analysis of BCAA levels

Sample preparation. Cells ($1x10^6$) from three independent biological replicates per treatment group were collected and washed twice with ice-cold PBS. Then, 1 ml of pre-chilled methanol/acetonitrile (8:2; v/v) solution was added. Each biological sample was prepared in duplicate as technical replicates for liquid chromatography-mass spectrometry (LC-MS) analysis. The cells were disrupted by sonication on ice (300 W; 5 min) and incubated at -20˚C for 30 min. After

centrifugation at ~15,000 x g for 15 min at 4˚C, the supernatant was collected, dried under nitrogen stream at a flow rate of 10-15 l/min and reconstituted in 100 μl acetonitrile: water (1:1; v/v). The sample was filtered through a 0.22-μm membrane prior to LC-MS analysis.

LC-MS conditions. i) Chromatographic conditions. Column: ACQUITY ultra performance liquid chromatography HSS T3 (2.1x100 mm; 1.8 μm; Waters Corporation); mobile phase: i) 0.1% formic acid in water; and ii) 0.1% formic acid in acetonitrile; flow rate: 0.3 ml/min; column temperature: 40˚C; injection volume: 2 μl. The gradient elution program was as follows: i) 0-2 min, 5-30% B; ii) 2-8 min, 30-100% B; iii) 8-10 min, 100-5% B; and iv) 10.1-12 min, 5% B.

ii) Mass spectrometric conditions. Ion source, electrospray ionization; scanning mode, positive ion mode; capillary voltage, 3.0 kV; nebulizer pressure, 40 psi; source temperature, 150˚C; desolvation temperature, 500˚C; desolvation gas flow, 1,000 l/h; cone gas flow, 50 l/h; scan range, 50-1,000 m/z; collision energy, 20 eV.

Statistical analysis. All experiments were performed with at least three independent biological replicates (n=3), each with three technical replicates. Data are presented as mean ± SD. Statistical analysis was performed using GraphPad Prism software (version 8.0; Dotmatics). Comparisons between two groups were conducted using two-tailed unpaired Student's t-test. For multiple-group comparisons, one-way ANOVA followed by Tukey's post hoc test was used to adjust for multiple comparisons.

For functional assays (wound healing and Transwell), data were analyzed using two-way ANOVA followed by Bonferroni's post hoc test to evaluate the main effects of AS-IV concentration and BCAT1 modification, as well as their interaction. To compare the efficacy of AS-IV across different genetic backgrounds, data were also normalized to the respective 0 μM control within each cell line group and expressed as percentage inhibition compared with the baseline. $P<0.05$ was considered to indicate a statistically significant difference. Specific statistical tests and exact P-values are indicated in the figure legends.

Results

Network pharmacology prediction of potential targets and pathways of AS-IV for breast cancer treatment. Using network pharmacology methods, a total of 524 potential targets of AS-IV were screened from databases including SwissTargetPrediction, while 5,250 breast cancer-associated targets were obtained from databases such as GeneCards, OMIM and DisGeNET. Of note, the 5,250 breast cancer-associated genes encompass a comprehensive collection of genes associated with breast cancer, including driver, tumor suppressor and other cancer-associated genes that may serve as biomarkers or therapeutic targets. After taking the intersection, 167 common candidate targets were identified (Fig. 1).

PPI network analysis and topological screening (using 'CytoHubba' and 'MCODE' plugins) revealed that targets such as BCAT1, AKT1, PIK3CA, EGFR and HSP90AA1 are located at the core of the network (Fig. 2A-C). Quantitative

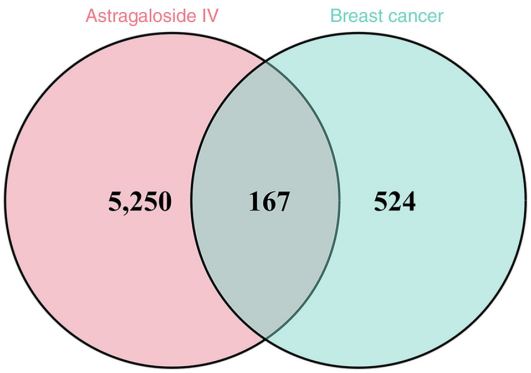

Figure 1. Venn diagram of overlapping core targets of astragaloside IV for triple-negative breast cancer.

ranking based on degree centrality identified the top 10 core targets, as presented in Table SII. Among these, HSP90AA1 and BCAT1 exhibited the highest degree values (both 46), followed by AKT1 with 40, EGFR with 39 and PIK3CA with 36, indicating their potential prominence in mediating the therapeutic effects of AS-IV against breast cancer. KEGG pathway enrichment analysis indicated that these core targets are significantly enriched in pathways such as 'pathways in cancer', 'proteoglycans in cancer', 'valine, leucine and isoleucine degradation', 'microRNAs in cancer' and 'Epstein-Barr virus infection' (Fig. 3).

GO functional enrichment analysis suggested that their biological processes mainly involve 'positive regulation of locomotion', 'cellular response to hormone stimulus', 'cellular response to lipid', 'regulation of hormone levels' and 'protein phosphorylation'. The analysis of cellular components primarily highlighted 'membrane raft', 'external side of plasma membrane', 'perinuclear region of cytoplasm', 'focal adhesion' and 'plasma membrane protein complex'. In terms of molecular function, the key enrichments included 'protein kinase activity', 'kinase binding', 'nuclear receptor activity', 'protein domain specific binding' and 'non-membrane spanning protein tyrosine kinase activity' (Fig. 4).

The further constructed comprehensive network diagram 'AS-IV-core targets-key pathways-breast cancer' visually illustrates the potential mechanism by which AS-IV exerts synergistic effects through multiple targets and pathways. As presented in Fig. 5, the network comprises 189 nodes and 986 edges. This analysis further identified key active components and core targets of AS-IV in the treatment of breast cancer. Among these, BCAT1 and the BCAA metabolic pathway emerged as key nodes within the network, providing a theoretical basis and direction for subsequent experimental research targeting BCAT1.

Establishment of BCAT1 KD and OE cell models. To investigate whether AS-IV influences breast cancer cell behavior through BCAT1, the present study transiently knocked down or overexpressed BCAT1 in MDA-MB-231 TNBC cells using siRNA and pcDNA3.1-BCAT1 plasmid, respectively. Transfection efficiency was validated 48 h post-transfection. Compared with the control and KD^{NC} groups (Fig. 6A-C), BCAT1 expression was significantly decreased in the KD^{BCAT1} group ($P<0.01$), indicating successful construction of the

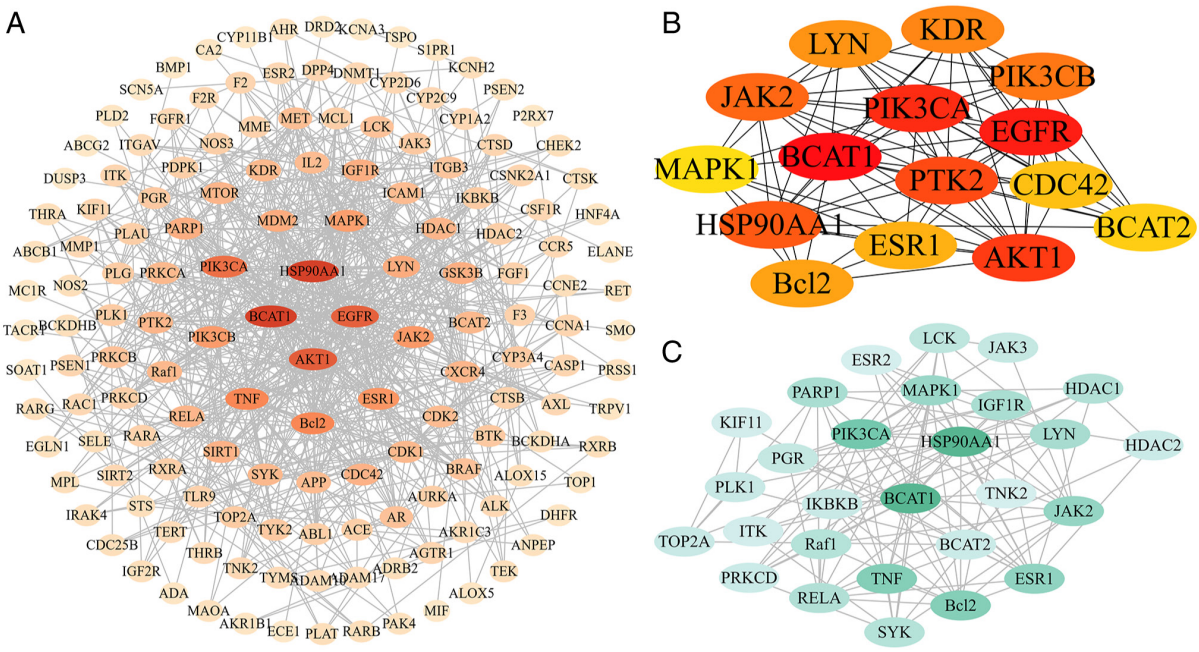

Figure 2. PPI network analysis and topological screening of AS-IV core targets. (A) PPI network diagram of astragaloside IV for triple-negative breast cancer. (B) Topological analysis by CytoHubba plugin. (C) Topological analysis by molecular complex detection. PPI, protein-protein interaction.

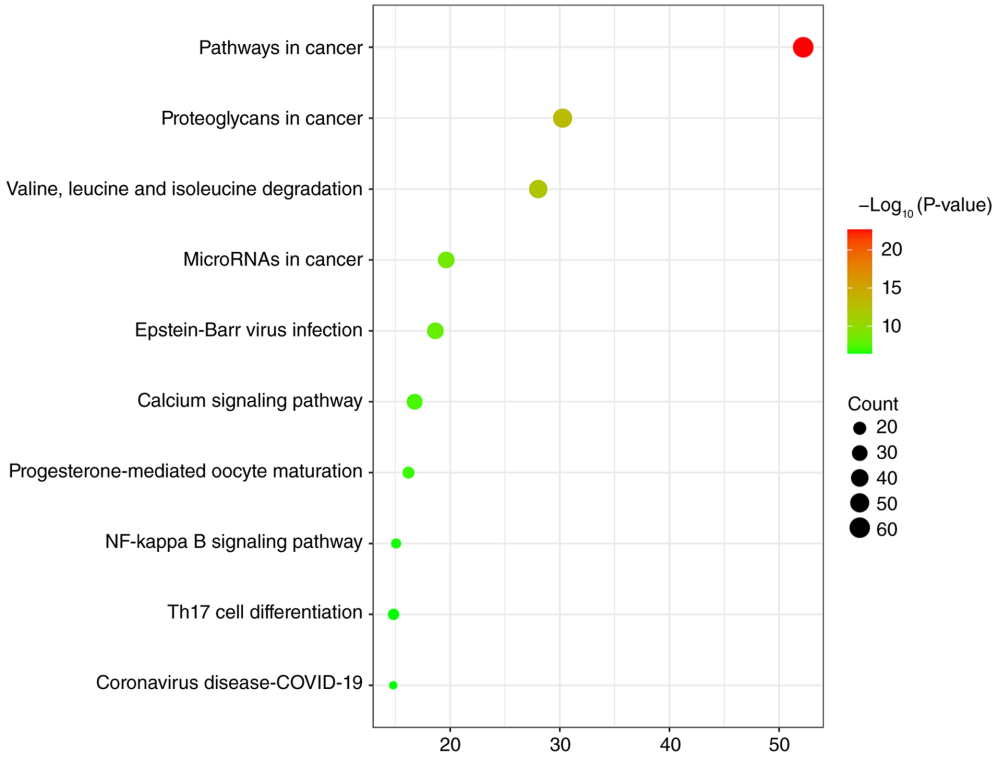

Figure 3. Kyoto Encyclopedia of Genes and Genomes pathway analysis of astragaloside IV for triple-negative breast cancer.

BCAT1-KD transiently transfected cells. Similarly, compared with the control and OE^{NC} groups (Fig. 6D-F), the OE^{BCAT1} group indicated a significant increase in BCAT1 expression ($P<0.01$), confirming the successful generation of the BCAT1-overexpressing transiently transfected cells.

Evidence of direct interaction between AS-IV and BCAT1. Molecular docking results demonstrated that AS-IV stably binds to BCAT1 with a predicted binding free energy of 8.4 kcal/mol, as calculated by AutoDock, indicating a strong binding affinity between the two molecules (Fig. 7B). The CETSA further revealed that AS-IV treatment markedly enhanced the thermal stability of BCAT1. As presented in Fig. 7A and C, in the untreated control group (NC), BCAT1 underwent notable thermal denaturation within the temperature range of 46-54˚C, accompanied by a marked decrease in

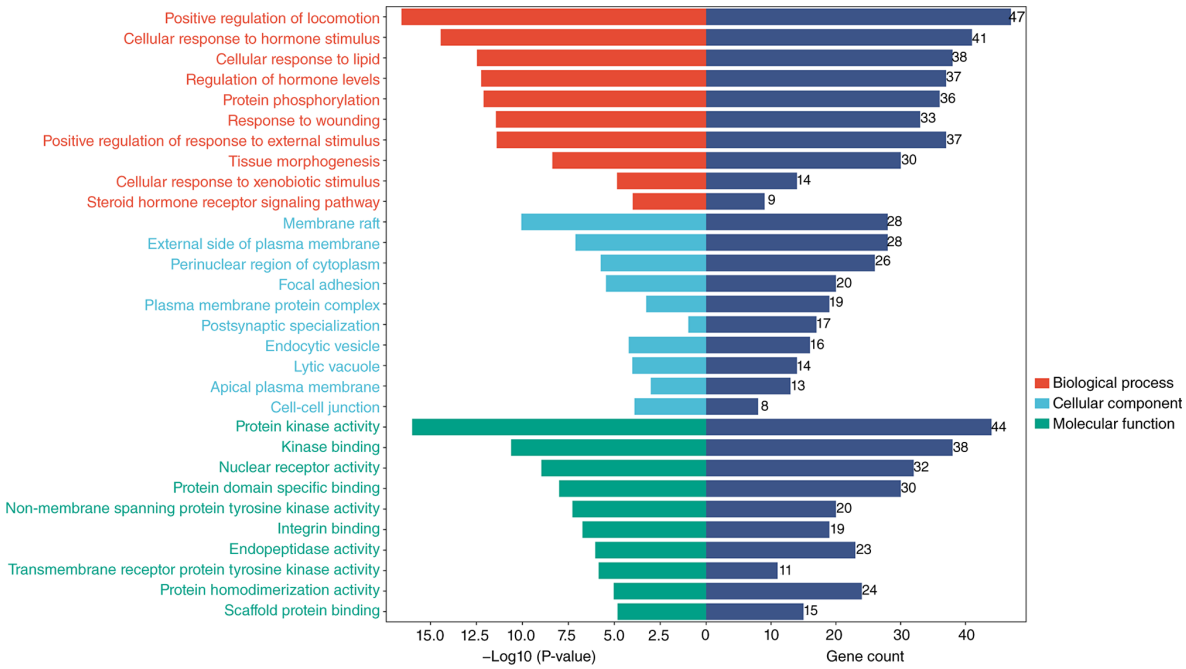

Figure 4. Gene Ontology functional enrichment analysis of astragaloside IV for triple-negative breast cancer.

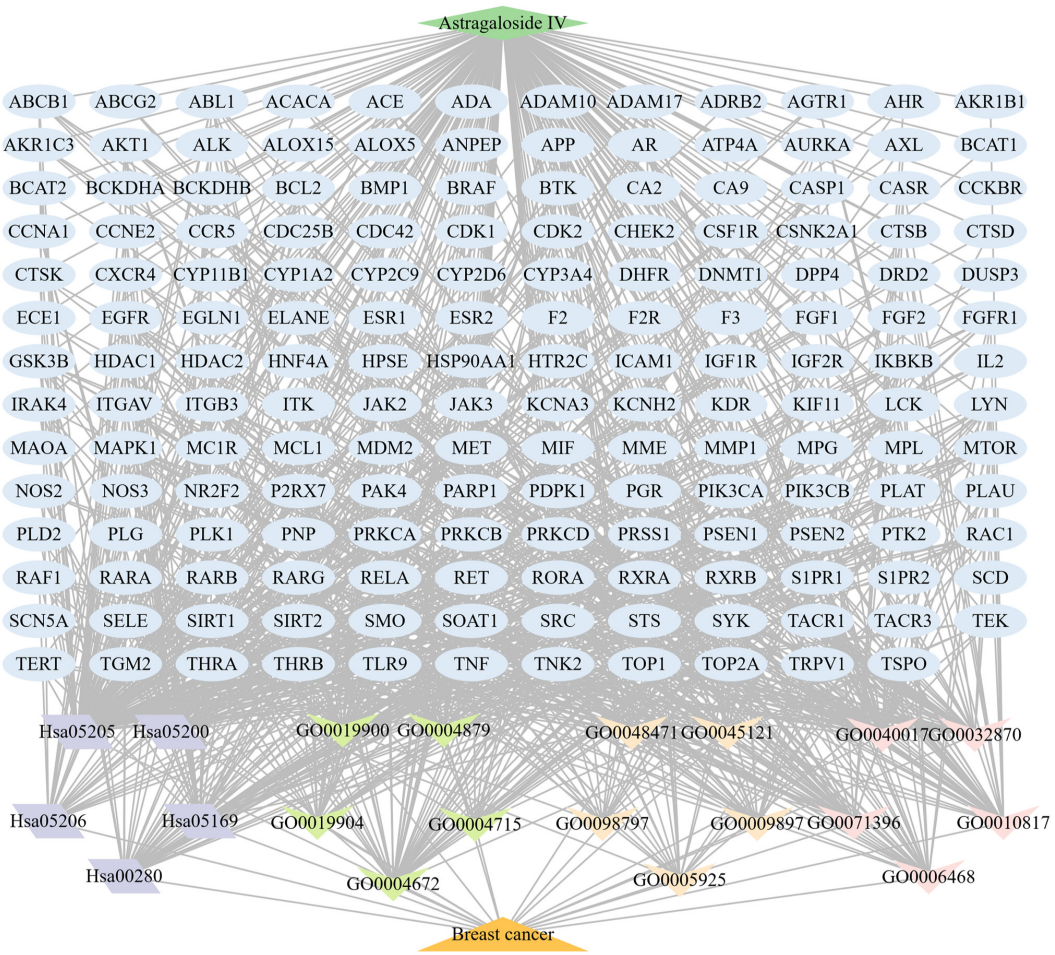

Figure 5. Network diagram of 'AS-IV-core targets-key pathways-breast cancer'.

solubility. By contrast, after treatment with 10 μM AS-IV for 1 h, the denaturation curve of BCAT1 shifted rightward and its melting temperature increased by 8˚C compared with the NC group (from 54 to 62˚C). These results suggested that AS-IV

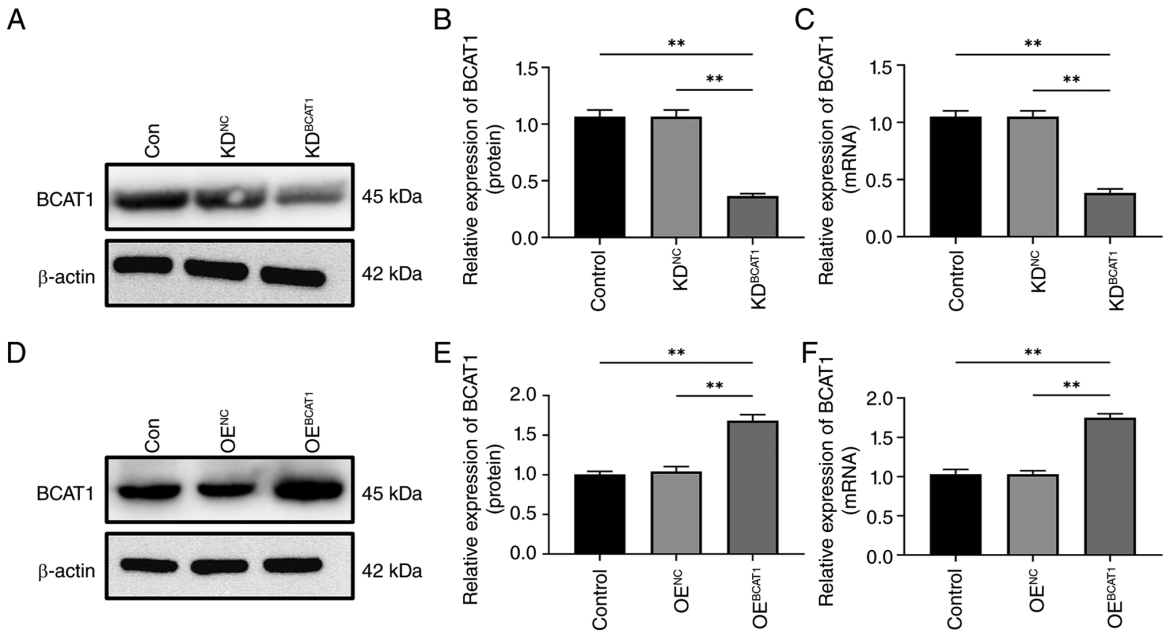

Figure 6. Validation of BCAT1 KD and OE cell models. (A) Western blot analysis of BCAT1 protein expression in BCAT1 KD cells. (B) Quantification of BCAT1 protein expression levels in BCAT1 KD cells. (C) Relative mRNA expression levels of BCAT1 in BCAT1 KD cells. (D) Western blot analysis of BCAT1 protein expression in BCAT1 OE cells. (E) Quantification of BCAT1 protein expression levels in BCAT1 OE cells. (F) Relative mRNA expression levels of BCAT1 in BCAT1 OE cells. **P<0.01. BCAT1, branched-chain amino acid transaminase 1; OE, overexpression; NC, negative control; KD, knockdown; Con, control.

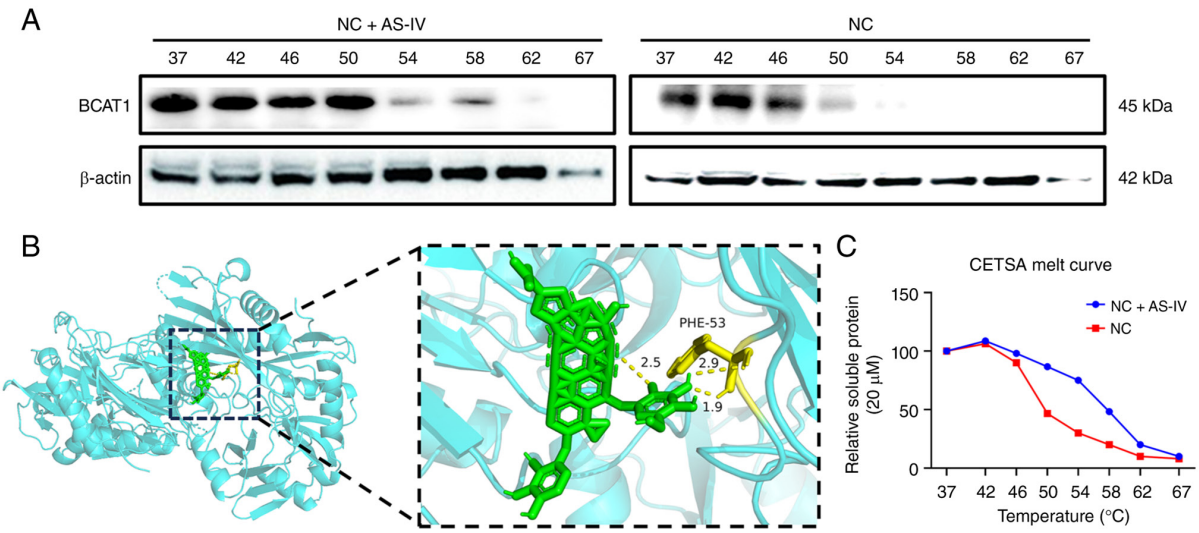

Figure 7. Direct interaction between AS-IV and BCAT1. (A) CETSA validation of the interaction between AS-IV and the BCAT1 protein. (B) Molecular docking simulation displaying the binding mode and predicted binding free energy between AS-IV and BCAT1. (C) Quantification of relative soluble protein levels from CETSA. Molecular weight markers (kDa) are indicated on the left of the blots: BCAT1 (43 kDa). NC, negative control; NC + AS-IV, negative control treated with AS-IV.

directly binds to BCAT1 under the investigated cellular conditions and enhances its thermal stability. This finding provided preliminary evidence of a physical interaction between AS-IV and BCAT1, supporting the hypothesis that BCAT1 may be a direct binding partner of AS-IV.

Effect of BCAT1 KD and OE on the anti-migratory activity of AS-IV in MDA-MB-231 TNBC cells. As presented in Fig. 8A and B (BCAT1 KD), two-way ANOVA revealed a significant main effect of AS-IV concentration [F(3, 16)=510.8; P<0.001], a significant main effect of BCAT1 modification [F(1, 16)=810.6; P<0.001] and a significant interaction between AS-IV concentration and BCAT1 modification [F(3, 16)=52.73; P<0.001] on wound closure. AS-IV treatment significantly reduced the relative wound area in both KD^{NC} and KD^{BCAT1} groups in a dose-dependent manner (Bonferroni post hoc test; all P<0.05). At each tested concentration, the KD^{BCAT1} group exhibited a more significant reduction in migration compared with the KD^{NC} group (P<0.001). As presented in Fig. 8C and D (BCAT1 OE), two-way ANOVA similarly

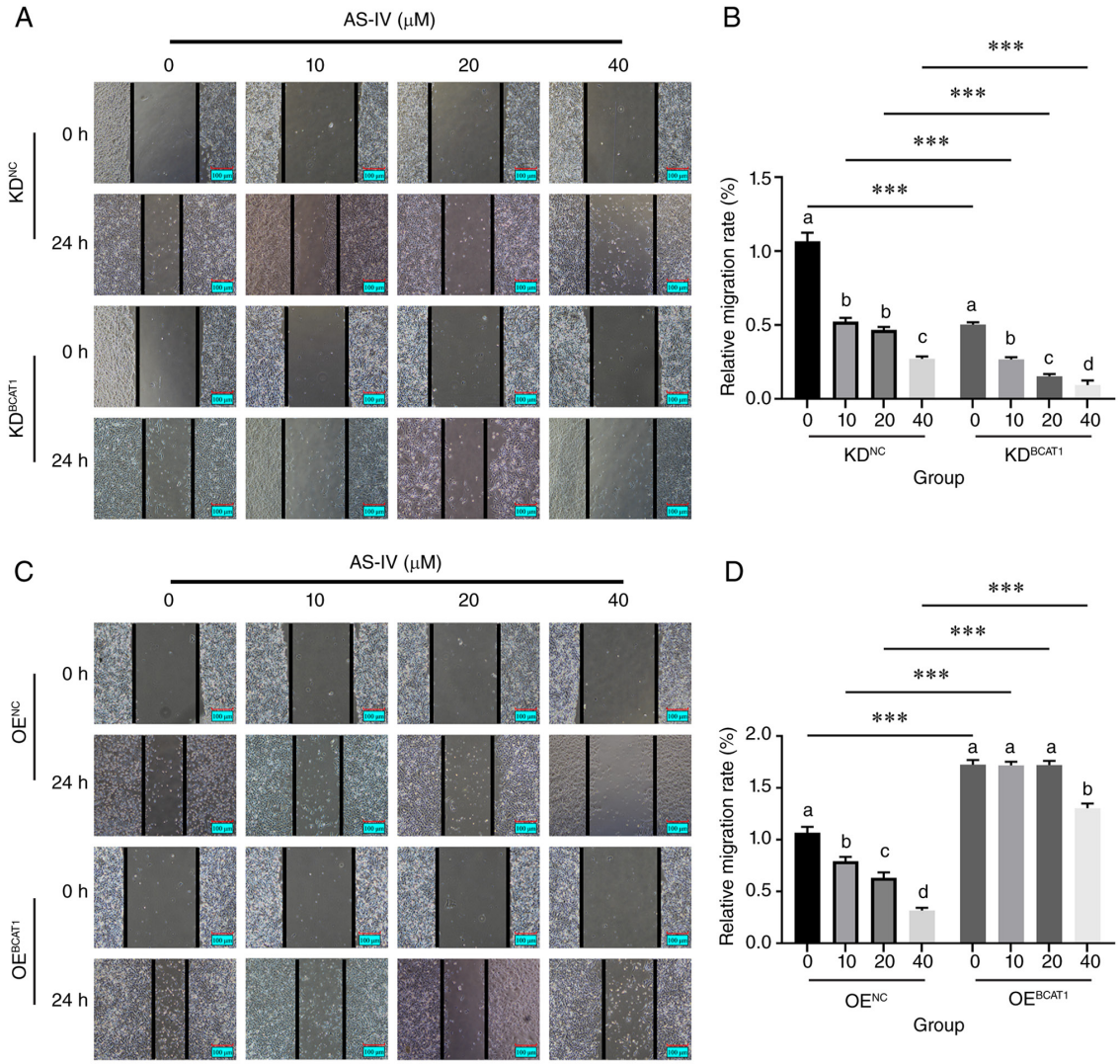

Figure 8. BCAT1 knockdown and overexpression modulate the anti-migratory effect of AS-IV in MDA-MB-231 triple-negative breast cancer cells. (A) Representative images of wound closure in MDA-MB-231 breast cancer cells with BCAT1 KD after treatment with different concentrations of AS-IV (0, 10, 20 and 40 μM) for 24 h. (B) Quantification of relative wound area in BCAT1 KD cells. x-axis: AS-IV concentration (μM). (C) Representative images of wound closure in MDA-MB-231 breast cancer cells with BCAT1 OE after treatment with different concentrations of AS-IV (0, 10, 20 and 40 μM) for 24 h. (D) Quantification of relative wound area in BCAT1 OE cells. x-axis: AS-IV concentration (μM). 'a', 'b', 'c' and 'd' represent the differences among different concentrations of AS-IV. There were no significant differences among groups sharing the same letters, while significant differences were observed between groups containing different letters (P<0.05). ***P<0.001. AS-IV, astragaloside-IV; BCAT1, branched-chain amino acid transaminase 1; OE, overexpression; NC, negative control; KD, knockdown.

demonstrated a significant main effect of AS-IV concentration [F(3, 16)=199.3; P<0.001], a significant main effect of BCAT1 modification [F(1, 16)=2667.5; P<0.001] and a significant interaction [F(3, 16)=27.02; P<0.001] on wound closure. AS-IV treatment decreased wound closure in both OE^{NC} and OE^{BCAT1} groups in a concentration-dependent manner (Bonferroni post hoc test; all P<0.05). Notably, at each concentration tested, the OE^{BCAT1} group demonstrated a significantly greater reduction in migration compared with the OE^{NC} group (P<0.05). These results demonstrated that AS-IV effectively suppresses cell migration in a concentration-dependent manner under both BCAT1 KD and OE conditions, albeit with altered efficacy depending on BCAT1 expression levels.

Effect of BCAT1 KD and OE on the anti-invasive activity of AS-IV in MDA-MB-231 TNBC cells. As presented in Fig. 9A and B (BCAT1 KD), two-way ANOVA revealed a significant main effect of AS-IV concentration [F(3, 16)=138.0; P<0.001], a significant main effect of BCAT1 modification [F(1, 16)=421.4; P<0.001] and a significant interaction between AS-IV concentration and BCAT1 modification [F(3, 16)=20.9; P<0.001] on cell invasion. AS-IV treatment significantly reduced the number of invaded cells in both KD^{NC} and KD^{BCAT1} groups in a dose-dependent manner (Bonferroni post hoc test, all P<0.05). At each concentration tested, the KD^{BCAT1} group exhibited a more significant decrease in cell invasion compared with the KD^{NC} group (P<0.05). As presented in Fig. 9C and D (BCAT1 OE), two-way ANOVA demonstrated a significant main effect of AS-IV concentration [F(3, 16)=129.8; P<0.001], a significant main effect of BCAT1 modification [F(1, 16)=160.0; P<0.001] and a significant interaction between AS-IV concentration and BCAT1 modification [F(3, 16)=3.06; P<0.001] on cell invasion. AS-IV treatment significantly decreased cell invasion in both OE^{NC} and OE^{BCAT1}

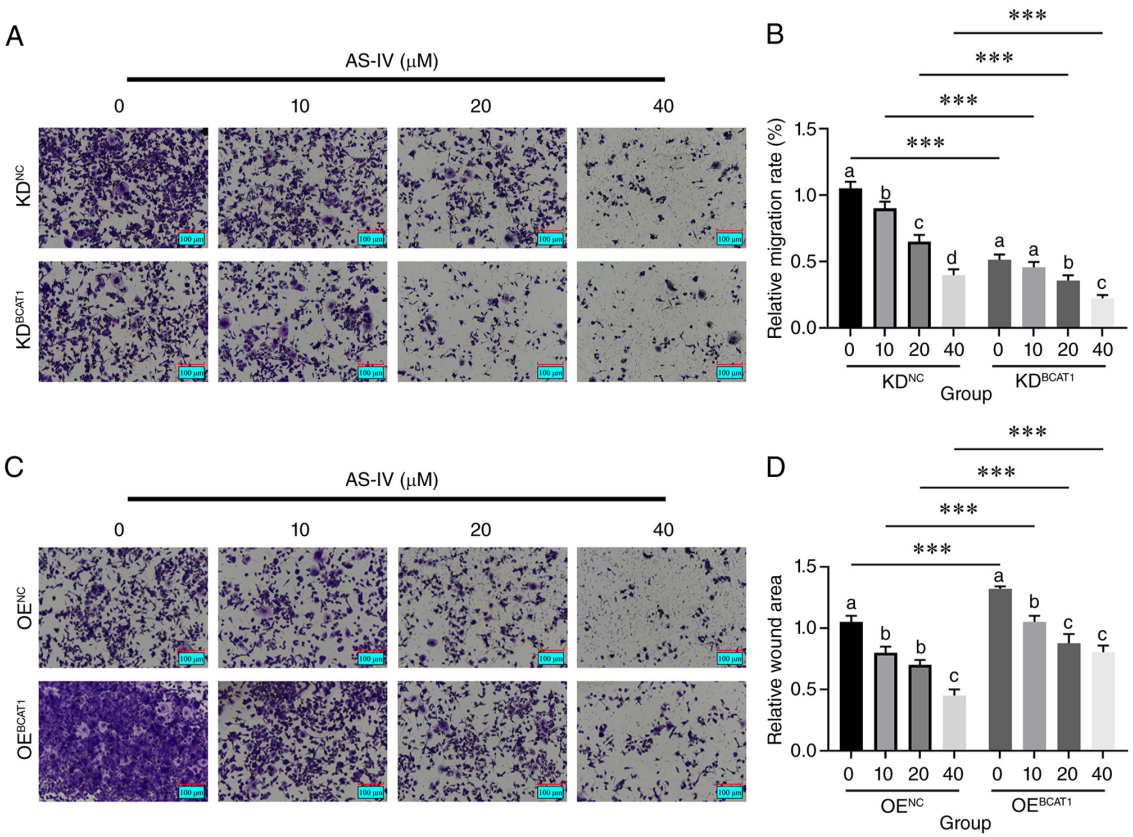

Figure 9. Effects of BCAT1 KD and OE on AS-IV-inhibited cell invasion by Transwell assay (scale bar, 100 μm). Representative images and statistical analysis of invading cells through Matrigel in MDA-MB-231 breast cancer cells with BCAT1 KD (A and B) or OE (C and D) after treatment with different concentrations of AS-IV (0, 10, 20 and 40 μM) for 24 h. For the knockdown groups, the interaction was significant (P<0.001). 'a', 'b', 'c' and 'd' represent the differences among different concentrations of AS-IV. There were no significant differences among groups sharing the same letters, while significant differences were observed between groups containing different letters (P<0.05). ***P<0.001. AS-IV, astragaloside-IV; BCAT1, branched-chain amino acid transaminase 1; OE, overexpression; NC, negative control; KD, knockdown.

groups in a concentration-dependent manner (Bonferroni post hoc test, all P<0.05). At each concentration tested, the OE^{BCAT1} group demonstrated a significantly greater reduction in cell invasion compared with the OE^{NC} group (P<0.05). These results indicated that AS-IV potently suppresses the invasive capacity of MDA-MB-231 TNBC cells in a concentration-dependent manner, and that BCAT1 expression levels modulate the efficacy of AS-IV.

Effects of AS-IV on the expression levels of BCAT1 downstream and associated proteins in MDA-MB-231 TNBC cells. Following BCAT1 KD in MDA-MB-231 TNBC cells, AS-IV treatment influenced the expression levels of BCAT1 downstream and associated proteins, as illustrated in Fig. 10. The results revealed that BCAT1 KD induced compensatory upregulation of BCAT2 compared with the NC (KD^{NC}) group (P<0.001). Regarding the branched-chain α-ketoacid dehydrogenase kinase (BCKDK)/branched-chain keto acid dehydrogenase E1 subunit β (BCKDHB) pathway, BCAT1 KD significantly reduced BCKDK activity compared with the KD^{NC} group (P<0.01), thereby alleviating its inhibitory effect on BCKDHB and leading to significantly increased basal BCKDHB activity compared with the KD^{NC} group (P<0.001). AS-IV intervention further enhanced this trend in a dose-dependent manner, directly inhibiting BCKDK activity and more potently activating BCKDHB.

OE^{BCAT1} resulted in compensatory downregulation of BCAT2 compared with the OE^{NC} group (P<0.001). Functionally, BCAT1 OE significantly enhanced BCKDK activity compared with the OE^{NC} group, thereby suppressing BCKDHB activity AS-IV treatment effectively counteracted the hyperactivation of BCKDK in a dose-dependent manner, partially reversing the inhibition of BCKDHB activity. However, under BCAT1 OE conditions, the extent of BCKDHB activity restoration by AS-IV did not reach the level observed in the NC group, suggesting that the high branched-chain α-keto acids environment resulting from OE^{BCAT1} partially attenuated the efficacy of AS-IV.

AS-IV promotes BCAA catabolism by modulating the BCAT1/BCKDK/BCKDH axis. The results indicated that KD^{BCAT1} significantly increased intracellular levels of BCAAs, including leucine, isoleucine and valine, compared with the NC group (P<0.001). This accumulation confirmed that BCAT1 is the rate-limiting enzyme for BCAA transamination; its downregulation creates a metabolic bottleneck upstream, impairing the initial step of BCAA catabolism. All three BCAAs exhibited a consistent dose-dependent accumulation (0, 10, 20 and 40 μM; P<0.01) (Fig. 11).

By contrast, OE^{BCAT1} itself significantly reduced the basal intracellular levels of leucine, isoleucine and valine compared with the NC group (P<0.001). AS-IV further enhanced BCAA

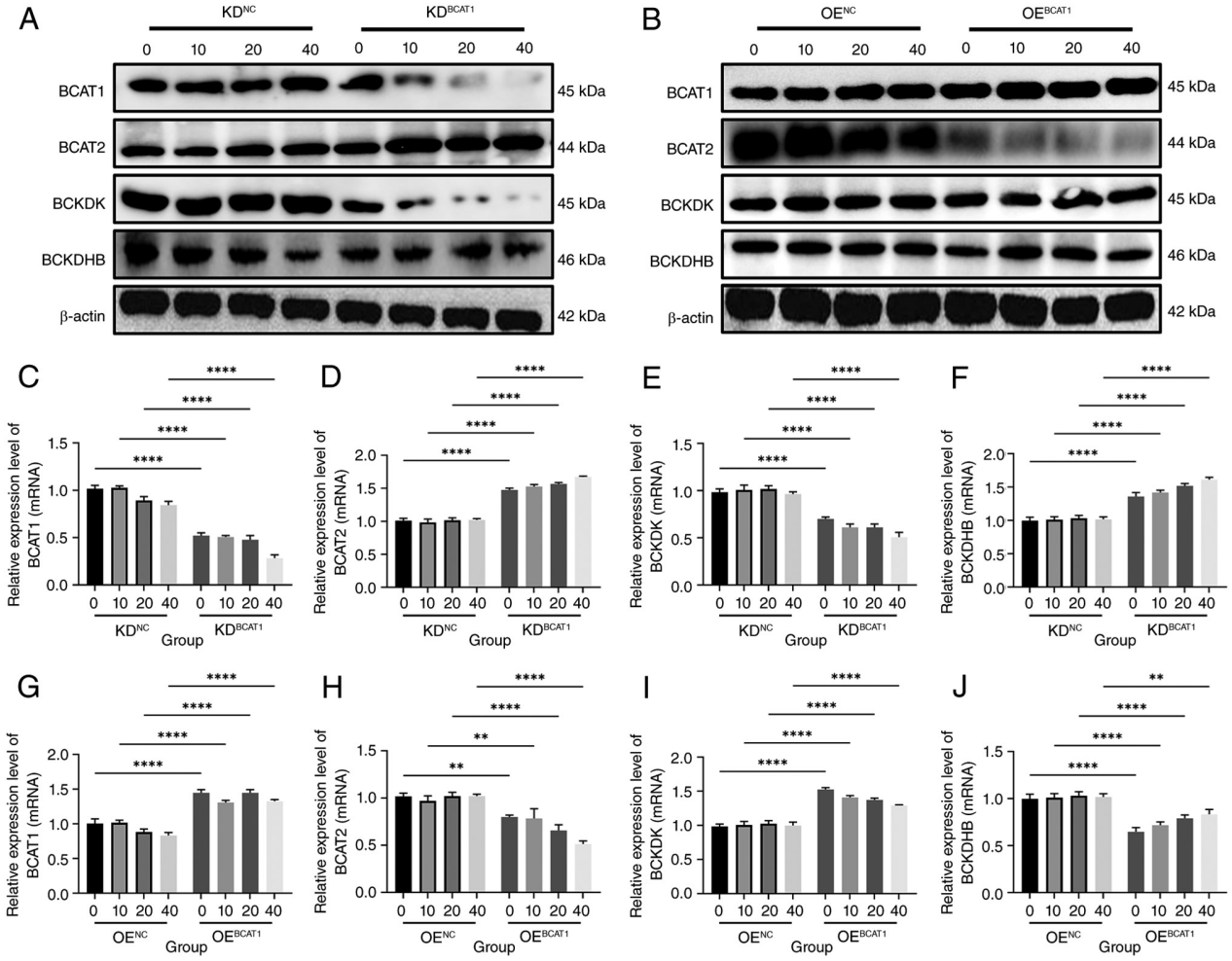

Figure 10. Effects of AS-IV on the expression levels of BCAT1 downstream and associated proteins in MDA-MB-231 TNBC cells. (A) Western blot analysis of BCAT2, BCKDK, BCKDHB and β-actin protein expression in BCAT1 KD cells. (B) Western blot analysis of BCAT2, BCKDK, BCKDHB and β-actin protein expression in BCAT1 OE cells. (C) Relative expression level of BCAT2 mRNA in BCAT1 KD cells. (D) Relative expression level of BCKDK mRNA in BCAT1 KD cells. (E) Relative expression level of BCKDHB mRNA in BCAT1 KD cells. (F) Relative expression level of BCAT1 mRNA in BCAT1 KD cells. (G) Relative expression level of BCAT2 mRNA in BCAT1 OE cells. (H) Relative expression level of BCKDK mRNA in BCAT1 OE cells. (I) Relative expression level of BCKDHB mRNA in BCAT1 OE cells. (J) Relative expression level of BCAT1 mRNA in BCAT1 OE cells. β-actin was used as the internal control. Data are presented as mean ± SD (n=3). **P<0.01 and ****P<0.0001 indicate significant differences compared with the respective control group (0 μM AS-IV) within the same genetic background. BCAT, branched-chain amino acid transaminase; OE, overexpression; NC, negative control; KD, knockdown; BCKDK, branched-chain α-ketoacid dehydrogenase kinase; BCKDHB, branched-chain keto acid dehydrogenase E1 subunit β.

degradation in a dose-dependent manner (0, 10, 20 and 40 μM; P<0.01) in both groups. Of note, in the OE group, due to the higher abundance of the BCAT1 target protein, the efficacy of AS-IV was markedly enhanced. The amino acid-lowering effect of AS-IV was significantly stronger in the OE group compared with that in the contemporaneous NC group (P<0.001), demonstrating a notable synergistic effect (Fig. 11).

Discussion

The present study provided evidence for a mechanism by which AS-IV inhibits the migration and invasion of MDA-MB-231 TNBC cells, potentially by targeting BCAT1 and modulating BCAA metabolism. Notably, these findings were derived from a single cell line model and thus represent preclinical evidence specific to this TNBC cell type. The present study findings not only provide a novel metabolic perspective on the antitumor effects of AS-IV but also offer experimental evidence suggesting BCAT1 as a potential therapeutic target for further investigation in oncology.

In recent years, numerous studies have highlighted the key role of metabolic reprogramming in tumor progression, with increasing attention focusing on aberrant amino acid metabolism (37-41). As essential amino acids, BCAAs are not only involved in protein synthesis but also function as signaling molecules regulating pro-tumor pathways such as mTOR complex 1 (42). BCAT1, the rate-limiting enzyme in BCAA catabolism, has been reported to be markedly expressed in various malignancies (for example, glioma and acute myeloid leukemia) and promotes tumor growth by maintaining intracellular BCAA levels (43). However, the role and underlying mechanisms of BCAT1 in breast cancer, particularly TNBC, remain to be elucidated. The present study demonstrated that BCAT1 expression significantly influences the migratory and invasive capabilities of MDA-MB-231 TNBC cells, which is consistent with its reported pro-metastatic roles in other malignancies. To the best of our knowledge, the present study

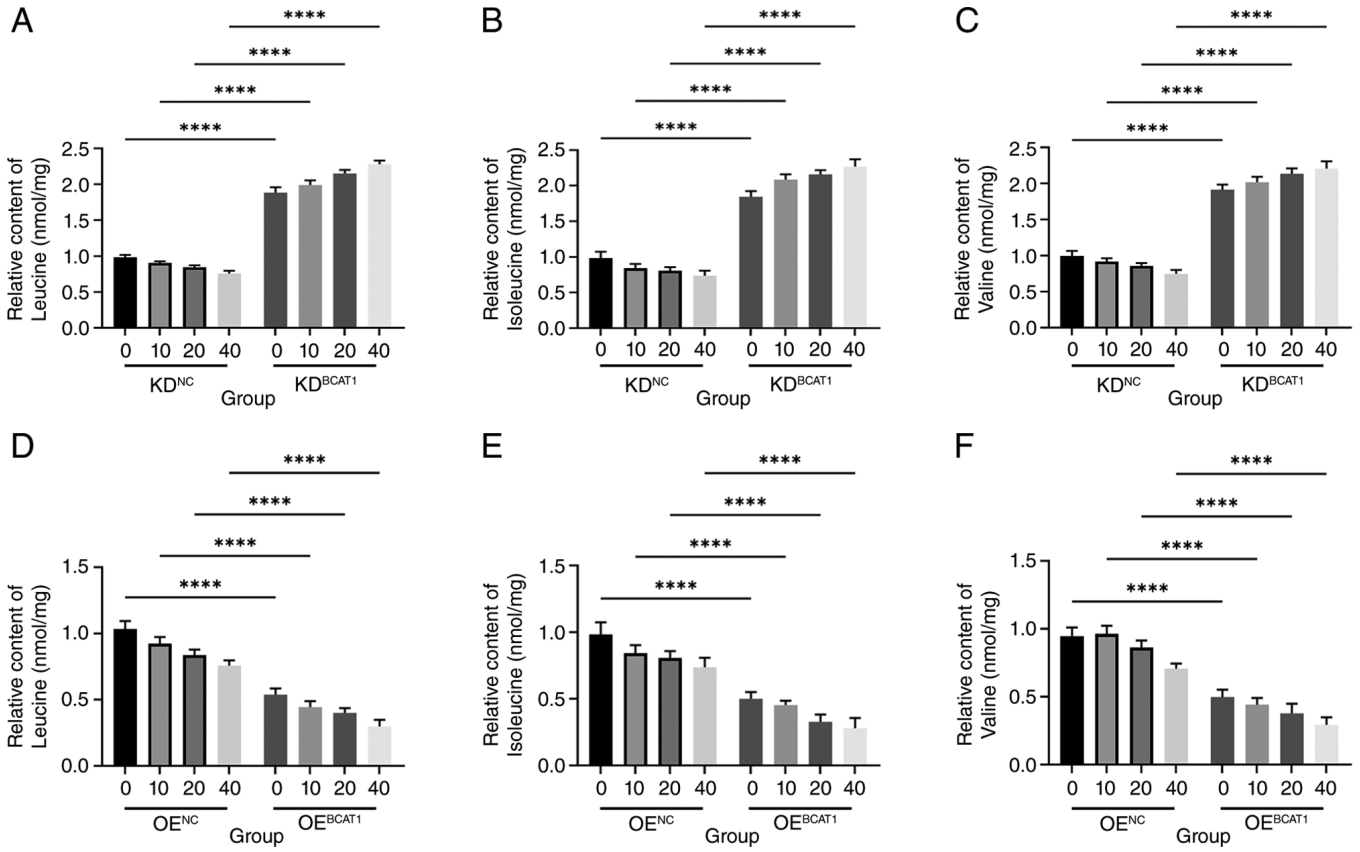

Figure 11. Intracellular branched-chain amino acid levels detected by liquid chromatography-mass spectrometry. (A) Relative changes in the intracellular content of leucine in MDA-MB-231 TNBC cells with BCAT1 KD after treatment with different concentrations of AS-IV (0, 10, 20 and 40 μM) for 24 h. (B) Relative changes in the intracellular content of isoleucine in MDA-MB-231 TNBC cells with BCAT1 KD after treatment with different concentrations of AS-IV (0, 10, 20 and 40 μM) for 24 h. (C) Relative changes in the intracellular content of valine in MDA-MB-231 TNBC cells with BCAT1 KD after treatment with different concentrations of AS-IV (0, 10, 20 and 40 μM) for 24 h. (D) Relative changes in the intracellular content of leucine in MDA-MB-231 TNBC cells with BCAT1 OE after treatment with different concentrations of AS-IV (0, 10, 20 and 40 μM) for 24 h. (E) Relative changes in the intracellular content of isoleucine in MDA-MB-231 TNBC cells with BCAT1 OE after treatment with different concentrations of AS-IV (0, 10, 20 and 40 μM) for 24 h. (F) Relative changes in the intracellular content of valine in MDA-MB-231 TNBC cells with BCAT1 OE after treatment with different concentrations of AS-IV (0, 10, 20 and 40 μM) for 24 h. ****P<0.0001 indicate significant differences compared with the respective control group (0 μM AS-IV) within the same genetic background. OE, overexpression; BCAT1, branched-chain amino acid transaminase 1; NC, negative control; KD, knockdown; AS-IV, astragaloside IV.

findings provide the first evidence that associates AS-IV, a natural compound from traditional Chinese medicine, with the regulation of BCAT1-mediated BCAA metabolism in breast cancer cells (44).

A key finding of the present study was that AS-IV binds to the BCAT1 protein and enhances its thermal stability, indicating a possible direct interaction. Both molecular docking and CETSA experiments consistently indicated a potential interaction between AS-IV and BCAT1, with computational prediction of high binding affinity and experimental observation of increased protein thermal stability. It is key to note that while CETSA provides evidence of target engagement in cell lysates and molecular docking predicts potential binding modes, these techniques are suggestive rather than definitive in establishing direct physical binding. Further validation using orthogonal approaches such as surface plasmon resonance (SPR) or isothermal titration calorimetry (ITC) would be key to confirm the direct interaction and determine binding kinetics. Furthermore, the specific amino acid residues mediating the AS-IV-BCAT1 interaction predicted by molecular docking have not been experimentally validated. Future studies employing site-directed mutagenesis of these key residues, combined with binding affinity measurements and enzymatic activity assays, are warranted to definitively establish the interaction interface and elucidate how AS-IV binding modulates BCAT1 catalytic function. It is key to clarify the directionality of this interaction and its functional consequences. The present study data indicated that AS-IV binding to BCAT1 does not simply 'activate' the enzyme in a binary manner; by contrast, it modulates the activity of the enzyme within the context of the entire BCAA metabolic pathway. Specifically, AS-IV promotes the flux of BCAAs through the catabolic pathway by influencing the downstream BCKDK/BCKDH axis, leading to enhanced BCAA degradation and reduced intracellular BCAA levels. This reduction in BCAA availability, therefore, attenuates pro-migratory and -invasive signaling (for example, the mTOR pathway), thereby suppressing malignant phenotypes. Thus, AS-IV functions as a metabolic modulator that redirects BCAA metabolism toward complete catabolism, rather than increasing or decreasing BCAT1 enzymatic activity. This identification provides a novel example of how natural compounds can exert antitumor effects through direct modulation of metabolic enzymes. While previous research has largely focused on the immunomodulatory and apoptosis-inducing effects

of AS-IV, the present study revealed a novel mechanism by which it exerts antitumor activity through targeting amino acid metabolic enzymes (45,46).

At the functional level, the present study confirmed that AS-IV markedly inhibits the migration and invasion of MDA-MB-231 TNBC cells in a concentration-dependent manner. Analysis of relative inhibition, normalized to the baseline of each group, revealed that BCAT1 expression levels modulate AS-IV efficacy: BCAT1 KD significantly attenuated the anti-migratory and -invasive effects of AS-IV (as reflected by reduced percentage inhibition), whereas BCAT1 OE enhanced AS-IV efficacy (increased percentage inhibition). These findings supported the notion that BCAT1 is a key mediator of the functional effects of AS-IV. Notably, AS-IV still exhibited significant dose-dependent inhibitory effects in BCAT1 KD cells, albeit to a lesser extent, suggesting that additional mechanisms may also contribute to its anti-migratory activity, consistent with its reported multi-target properties (15,18,22,47-49).

Mechanistically, the present study revealed that BCAT1 expression significantly influences the activity of the downstream BCKDK/BCKDH pathway and intracellular BCAA accumulation. AS-IV treatment further enhanced BCKDHB activation induced by BCAT1 KD and partially reversed BCKDHB suppression resulting from BCAT1 OE. This bidirectional regulatory capacity, enhancing BCKDHB activity when it is basally low (as in KD cells) and partially restoring it when it is suppressed (as in OE cells), suggests that AS-IV acts as a modulator of pathway flux rather than a simple agonist or antagonist of BCAT1 enzymatic activity. By promoting the complete oxidation of BCAAs via the BCKDHB complex, AS-IV reduces the intracellular pool of these amino acids, thereby limiting their availability to promote pro-metastatic signaling pathways. Notably, AS-IV demonstrated a stronger BCAA-lowering effect in BCAT1-overexpressing cells compared with the NC (OE^{NC}) group, indicating that its efficacy is closely associated with BCAT1 protein levels. The present study finding is consistent with the established central role of the BCAT1/BCKDK axis in amino acid metabolism but proposes AS-IV as a positive modulator of this pathway (50,51).

From the perspective of metabolic reprogramming, BCAAs not only provide substrates for protein synthesis but also act as nutrient signals that activate pro-tumor pathways such as mTOR (52). The present study suggested that by promoting BCAA degradation and reducing their intracellular levels, AS-IV may indirectly suppress associated oncogenic signaling pathways such as the mTOR pathway. This aligns with previous studies on the role of the BCAA-mTOR axis in tumor progression (53-56); however, to the best of our knowledge, the present study is the first to directly associate a natural monomer compound derived from traditional Chinese medicine with this pathway, thereby providing a theoretical foundation for the application of metabolic intervention strategies in breast cancer treatment in the future.

However, the present study has certain limitations. All experiments were conducted solely in cellular models and the anti-metastatic effects of AS-IV mediated through BCAT1 have not yet been validated in animal models. Furthermore, the expression patterns and clinical significance of BCAT1 across different molecular subtypes of breast cancer remain to be fully elucidated. Future studies should focus on establishing breast cancer migration animal models to evaluate the *in vivo* efficacy and potential toxicity of AS-IV, in addition to conducting correlation analyses based on clinical samples to facilitate its translational applications. Second, the present study was conducted exclusively in the MDA-MB-231 TNBC cell line. While TNBC represents an aggressive subtype with high clinical relevance, the absence of other breast cancer subtypes (for example, hormone $receptor^{+}$ MCF-7 or HER2-amplified SKBR3 cells) limits the generalizability of the present study findings. BCAT1 expression and BCAA metabolic patterns may differ across breast cancer molecular subtypes and whether AS-IV exerts similar effects in these contexts remains to be investigated in future research. Third, although the molecular docking and CETSA experiments in the present study suggested a potential direct interaction between AS-IV and BCAT1, the evidence remains indirect and preliminary. The predicted binding mode has not been validated using site-directed mutagenesis of key amino acid residues and the precise effect of AS-IV binding on BCAT1 enzymatic activity has not been directly measured. Such validation, including mutagenesis studies combined with SPR or ITC to assess binding kinetics, as well as enzymatic activity assays, is key to definitively establishing BCAT1 as a direct molecular target of AS-IV and to understand the functional consequences of their interaction.

In conclusion, the present study indicated that AS-IV suppresses the migration and invasion of MDA-MB-231 TNBC cells and that this effect may involve targeting BCAT1 and modulating BCAA metabolism in this *in vitro* cell model. AS-IV exhibits predicted high binding affinity to BCAT1 in molecular docking experiments and enhances the thermal stability of the protein in CETSA experiments, suggesting a potential direct interaction. Functionally, AS-IV inhibits migration and invasion of breast cancer cell in a concentration-dependent manner; although this effect is attenuated under BCAT1 KD or OE conditions, it remains statistically significant, indicating that BCAT1 is a key target of AS-IV. Mechanistically, AS-IV promotes BCAA catabolism by modulating BCKDK/BCKDH pathway activity, thereby lowering intracellular BCAA levels and therefore, suppressing oncogenic signaling cascades such as the mTOR axis. To the best of our knowledge, the present study findings, for the first time, associated an active component of traditional Chinese medicine with a metabolic enzyme target and the malignant phenotype of MDA-MB-231 TNBC cells, not only expanding the antitumor mechanistic repertoire of AS-IV but also offering a potential mechanistic rationale for future exploration of BCAA-centric metabolic intervention in this cell model. Further studies in diverse breast cancer models are warranted to determine the generalizability of these observations. Further investigations in pre-clinical animal models and clinical specimens are warranted to validate the *in vivo* efficacy and translational potential of this mechanism.

Acknowledgements

Not applicable.

Funding

The present study was supported by the Shaanxi Provincial Department of Science and Technology (grant nos 2025JC-YBMS-903 and 2023-JC-QN-0995) and Yan'an Science and Technology Plan Project (grant no. 2022SLSFGG-019).

Availability of data and materials

The data generated in the present study are not publicly available due restrictions by the institutional data management policy and the collaborative research agreement but may be requested from the corresponding author.

Authors' contributions

YTL conceived and designed the research studies and contributed markedly to data interpretation, manuscript writing and final approval of the manuscript. LZ analyzed experimental data and contributed to manuscript writing and revisions. XDS contributed to data acquisition, analysis and interpretation, and critically revised the manuscript for important intellectual content. All authors read and approved the final manuscript. YTL and XDS confirm the authenticity of all the raw data.

Ethics approval and consent to participate

Not applicable.

Patient consent for publication

Not applicable.

Competing interests

The authors declare that they have no competing interests.

References

1. Akizawa Y, Kanno T, Horibe Y, Shimizu Y, Noguchi E, Yamamoto T, Okamoto T, Nagashima Y and Tabata T: Ovarian metastasis from breast cancer mimicking a primary ovarian neoplasm: A case report. Mol Clin Oncol 15: 135, 2021.
2. Kim J, Harper A, McCormack V, Sung H, Houssami N, Morgan E, Mutebi M, Garvey G, Soerjomataram I and Fidler-Benaoudia MM: Global patterns and trends in breast cancer incidence and mortality across 185 countries. Nat Med 31: 1154-1162, 2025.
3. World Health Organization (WHO): Breast cancer. WHO fact sheet. WHO, Geneva, 2024.
4. Kong F, Wang C, Zhang J, Wang X, Sun B, Xiao X, Zhang H, Song Y and Jia Y: Chinese herbal medicines for prostate cancer therapy: From experimental research to clinical practice. Chin Herb Med 15: 485-495, 2023.
5. Kong F, Wang C, Zhao L, Liao D, Wang X, Sun B, Yang P and Jia Y: Traditional Chinese medicines for non-small cell lung cancer: Therapies and mechanisms. Chin Herb Med 15: 509-515, 2023.
6. Tian Y, Ma B, Yu S, Li Y, Pei H, Tian S, Zhao X, Liu C, Zuo Z and Wang Z: Clinical antitumor application and pharmacological mechanisms of Dahuang Zhechong Pill. Chin Herb Med 15: 169-180, 2023.
7. Li S, Liu Y, Hu W, Deng A, Ren X, Chen L, Lu Y, Wu Y, Huang H, Cao J, *et al*: Protein lipoylation in cancer: Metabolic reprogramming and therapeutic potential. Cell Death Discov 11: 420, 2025.
8. Tanase DM, Valasciuc E, Costea CF, Scripcariu DV, Ouatu A, Hurjui LL, Tarniceriu CC, Floria DE, Ciocoiu M, Baroi LG and Floria M: Duality of branched-chain amino acids in chronic cardiovascular disease: Potential biomarkers versus active pathophysiological promoters. Nutrients 16: 1972, 2024.
9. Long L, Yang WS, Liu L, Tobias DK, Katagiri R, Wu K, Jin L, Zhang FF, Luo X, Liu X, *et al*: Dietary intake of branched-chain amino acids and survival after colorectal cancer diagnosis. Int J Cancer 148: 2471-2480, 2021.
10. Song Y, Zhao B, Xu Y, Ren X, Lin Y, Zhou L and Sun Q: Prognostic significance of branched-chain amino acid transferase 1 and CD133 in triple-negative breast cancer. BMC Cancer 20: 584, 2020.
11. Zhang L and Han J: Branched-chain amino acid transaminase 1 (BCAT1) promotes the growth of breast cancer cells through improving mTOR-mediated mitochondrial biogenesis and function. Biochem Biophys Res Commun 486: 224-231, 2017.
12. Thewes V, Simon R, Hlevnjak M, Schlotter M, Schroeter P, Schmidt K, Wu Y, Anzeneder T, Wang W, Windisch P, *et al*: The branched-chain amino acid transaminase 1 sustains growth of antiestrogen-resistant and ERα-negative breast cancer. Oncogene 36: 4124-4134, 2017.
13. Huang L, Li G, Zhang Y, Zhuge R, Qin S, Qian J, Chen R, Kwan Wong Y, Tang H, Wang P, *et al*: Small-molecule targeting BCAT1-mediated BCAA metabolism inhibits the activation of SHOC2-RAS-ERK to induce apoptosis of Triple-negative breast cancer cells. J Adv Res 75: 723-738, 2025.
14. Deng YP, Zhu H, Xing J, Gao J, Duan J, Liu P, Zhong G and Cai X: The role of natural products in improving lipid metabolism disorder-induced mitochondrial dysfunction of diabetic kidney disease. Front Physiol 16: 1624077, 2025.
15. Chen C, Bu X, Deng L, Xia J, Wang X, Chen L, Li W, Huang J, Chen Q and Wang C: Astragaloside IV as a promising therapeutic agent for liver diseases: Current landscape and future perspectives. Front Pharmacol 16: 1574154, 2025.
16. Xiong BB, Zhuo YM, Wang H, Zheng QL, Tang F, Huang Q and Yao M: Macrophage polarization in disease therapy: Insights from astragaloside IV and cycloastragenol. Front Pharmacol 16: 1598022, 2025.
17. Lai Y, Liu R, Shao H, Zhan J, Ma Y, Zhou L, Wan Z, Li S, Wang W, Jiang L and Shao Y: Mechanism of Astragaloside-Brucea javanica oil nanoemulsion against oral squamous cell carcinoma through CDK1/MTFR2: Network pharmacology, bioinformatics, and experimental studies. PLoS One 20: e0329622, 2025.
18. Gao X, Hao W, Wang Y, Wu X, Zhu F and Zhang Y: Molecular mechanisms of astragaloside-IV in hepatocellular carcinoma therapy: A systematic review. BMC Cancer 25: 1407, 2025.
19. Zeng Y, Duan T, Huang J and Wang X: Astragaloside IV inhibits nasopharyngeal carcinoma progression by suppressing the SATB2/Wnt signaling axis. Toxicol Res (Camb) 14: tfaf047, 2025.
20. Yin W, Liao X, Sun J, Chen Q and Fan S: Astragaloside IV inhibits the proliferation, migration, invasion, and epithelial-mesenchymal transition of oral cancer cells by aggravating autophagy. Tissue Cell 90: 102524, 2024.
21. Wang X, Gao S, Song L, Liu M, Sun Z and Liu J: Astragaloside IV antagonizes M2 phenotype macrophage polarization-evoked ovarian cancer cell malignant progression by suppressing the HMGB1-TLR4 axis. Mol Immunol 130: 113-121, 2021.
22. Hu C, Li Q, Gong SN, Zou XJ, Xu JY, Ying HF and Zheng L: Astragaloside IV: A potential nemesis for gastric cancer. Front Pharmacol 16: 1636341, 2025.
23. Yang Y, Lu J, Zhu Y, Chen D, Tang J, Zhang M, Lu J, Yang Y, Tian S and Zhao H: Astragaloside IV inhibits the growth of obesity-associated triple-negative breast cancer by activating FOXA1 transcription factor to regulate GAL3ST1-GalCer signaling and remodel sphingolipid metabolism. Phytomedicine 144: 156907, 2025.
24. Hopkins AL: Network pharmacology: The next paradigm in drug discovery. Nat Chem Biol 4: 682-690, 2008.
25. Guan Y, Cheng J, Lv Q, Wei X, Jiang B and Xiao P: Exploring new therapeutic potential of five commonly used Pteris medicinal plants through pharmaphylogenomics and network pharmacology. Chin Herb Med 17: 808-821, 2025.
26. Gao J, Han C, Dai N, Wang W, Jin T, Du D and Xia Q: Traditional Chinese medicine formulas alleviated acute pancreatitis via improvement of microcirculation: A systematic review and meta-analysis. Chin Herb Med 17: 584-600, 2024.
27. Shang L, Wang Y, Li J, Zhou F, Xiao K, Liu Y, Zhang M, Wang S and Yang S: Mechanism of Sijunzi Decoction in the treatment of colorectal cancer based on network pharmacology and experimental validation. J Ethnopharmacol 302 (Pt A): 115876, 2023.

28. Zhai Y, Liu L, Zhang F, Chen X, Wang H, Zhou J, Chai K, Liu J, Lei H, Lu P, *et al*: Network pharmacology: A crucial approach in traditional Chinese medicine research. Chin Med 20: 8, 2025.
29. Li L, Yang L, Yang L, He C, He Y, Chen L, Dong Q, Zhang H, Chen S and Li P: Network pharmacology: A bright guiding light on the way to explore the personalized precise medication of traditional Chinese medicine. Chin Med 18: 146, 2023.
30. Li X, Liu Z, Liao J, Chen Q, Lu X and Fan X: Network pharmacology approaches for research of Traditional Chinese Medicines. Chin J Nat Med 21: 323-332, 2023.
31. Tian JS, Wu ZN, Wu D, Yang C, Gao Y, Yan DL and Qin XM: Combining network pharmacology and experimental verification to reveal the mechanism of Chaigui granules in the treatment of depression through PI3K/Akt/mTOR signaling pathways. Metab Brain Dis 38: 2849-2864, 2023.
32. Paggi JM, Pandit A and Dror RO: The art and science of molecular docking. Annu Rev Biochem 93: 389-410, 2024.
33. Ansari RM, Mundke RN, Agrawal YO, Goyal SN, Nakhate KT and Rathod SS: Recent advances in molecular docking techniques: Transforming perspectives in distinct drug targeting and drug discovery approaches. Med Chem: Jul 21, 2025 (Epub ahead of print).
34. Abdul Kader S, Dib S, Achkar IW, Thareja G, Suhre K, Rafii A and Halama A: Defining the landscape of metabolic dysregulations in cancer metastasis. Clin Exp Metastasis 39: 345-362, 2022.
35. Biswas D, Slade L, Duffley L, Mueller N, Dao KT, Mercer A, Pakkiriswami S, El Hiani Y, Kienesberger PC and Pulinilkunnil T: Inhibiting BCKDK in triple negative breast cancer suppresses protein translation, impairs mitochondrial function, and potentiates doxorubicin cytotoxicity. Cell Death Discov 7: 241, 2021.
36. Livak KJ and Schmittgen TD: Analysis of relative gene expression data using real-time quantitative PCR and the 2(-Delta Delta C(T)) Method. Methods 25: 402-408, 2001.
37. Dong C, Zhang Y, Zeng J, Chong S, Liu Y, Bian Z, Fan S and Chen X: FUT2 promotes colorectal cancer metastasis by reprogramming fatty acid metabolism via YAP/TAZ signaling and SREBP-1. Commun Biol 7: 12972024, 2024.
38. Yu M, Yang D, Chen X, Yang Y, Zhang B, Jiang X, Xing L, Yang Y, Sun Y and Li N: Metabolic reprogramming in cancer: Dysregulation of glucose, lipid, and amino acid pathways and therapeutic opportunities. Mol Biomed 7: 25, 2026.
39. Huang K, Han Y, Chen Y, Shen H, Zeng S and Cai C: Tumor metabolic regulators: Key drivers of metabolic reprogramming and the promising targets in cancer therapy. Mol Cancer 24: 7, 2025.
40. Zhang J, Chen M, Yang Y, Liu Z, Guo W, Xiang P, Zeng Z, Wang D and Xiong W: Amino acid metabolic reprogramming in the tumor microenvironment and its implication for cancer therapy. J Cell Physiol 239: e31349, 2024.
41. Brown ML, Cai X and Simon MC: Branched chain amino acids and their aberrant metabolism in cancer. Trends Cancer 12: 34-47, 2026.
42. Zhao Z, Dong J, Wang D, Zhao C, Tian X, Meng Y, Zou Y, Zhao Y, Qin G, Wang T, *et al*: Metabolomic analysis of rumen-protected branched-chain amino acids in primiparous dairy cows. Front Immunol 15: 1385896, 2024.
43. Ling ZN, Jiang YF, Ru JN, Lu JH, Ding B and Wu J: Amino acid metabolism in health and disease. Signal Transduct Target Ther 8: 345, 2023.
44. Wang M, Zhang Y, Ni S, Sun M, Wu Q, Wu X, Chen Q and Wang S: The anti-cancer activity of Dioscin: An update and future perspective. Med Oncol 42: 63, 2025.
45. Xu F, Cui WQ, Wei Y, Cui J, Qiu J, Hu LL, Gong WY, Dong JC and Liu BJ: Astragaloside IV inhibits lung cancer progression and metastasis by modulating macrophage polarization through AMPK signaling. J Exp Clin Cancer Res 37: 207, 2018.
46. Tian L, Zhao JL, Kang JQ, Guo SB, Zhang N, Shang L, Zhang YL, Zhang J, Jiang X and Lin Y: Astragaloside IV alleviates the experimental DSS-Induced colitis by remodeling macrophage polarization through STAT signaling. Front Immunol 12: 740565, 2021.
47. Cui Z and Shang Q: Mechanistic insights into the antitumor effects of astragaloside IV and astragalus polysaccharide in digestive system cancers. Front Pharmacol 16: 1691011, 2025.
48. Liu S and Yu YW: Network pharmacology: Changes the treatment mode of 'one disease-one target' in cancer treatment. World J Gastrointest Oncol 17: 101581, 2025.
49. Li J, Qu Y, Zhang W, Yang Z, Zeng Y, Xu J, Xie K and Liu Q: Astragaloside IV targets TUBB4B to inhibit proliferation and promote apoptosis of pituitary tumor cells via the STMN1/ERK pathway. Int J Mol Med 57: 151, 2026.
50. Ivanova OA, Predeus AV, Sorokina MY, Ignatieva EV, Bobkov DE, Sukhareva KS, Kostareva AA and Dmitrieva RI: LMNA R482L mutation causes impairments in C2C12 myoblasts subpopulations, alterations in metabolic reprogramming during differentiation, and oxidative stress. Sci Rep 15: 5358, 2025.
51. Jishi A, Hu D, Shang Y, Wang R, Gunzler SA and Qi X: BCKDK loss impairs mitochondrial Complex I activity and drives alpha-synuclein aggregation in models of Parkinson's disease. Acta Neuropathol Commun 12: 198, 2024.
52. Holeček M: Branched-chain amino acids in health and disease: Metabolism, alterations in blood plasma, and as supplements. Nutr Metab (Lond) 15: 33, 2018.
53. Wang L, Shi F, Cao Y and Xie L: Multiple roles of branched-chain amino acid metabolism in tumour progression. J Biomed Sci 32: 41, 2025.
54. He B, Li L, Liu Y, Hao M, Zhang L and He R: BCAAs and related metabolic enzymes: Partners in crime driving tumor development. Front Cell Dev Biol 14: 1748587, 2026.
55. Xiong H, Liu R, Xu K, Chen X, Huang L, Shou Y, Huang Y, Sheng H, Lu Y and Zhang H: Branched-chain amino acid and cancer: Metabolism, immune microenvironment and therapeutic targets. J Transl Med 23: 636, 2025.
56. Zhou Y, Kou J, Li W, Wang Y, Su X and Zhang H: BCAA metabolism in cancer progression and therapy resistance: The balance between fuel and cell signaling. Front Pharmacol 16: 1595176, 2025.